Neutral pion photoproduction on nuclei in baryon chiral perturbation theory

S. R. Beane,[1,*] C. Y. Lee,[2,†] and U. van Kolck[3,‡]

[1]*Department of Physics, Duke University, Durham, North Carolina 27708*
[2]*Nuclear Theory Group, Department of Physics, The University of Texas, Austin, Texas 78712*
[3]*Department of Physics, Box 351560, University of Washington, Seattle, Washington 98195*
(Received 9 August 1995)

Threshold neutral pion photoproduction on light nuclei is studied in the framework of baryon chiral perturbation theory. We obtain a general formula for the electric dipole amplitude in the special case of neutral pion photoproduction on a nucleus. To third order in small momenta, the amplitude is a sum of 2- and 3-body interactions with no undetermined parameters. With reasonable input from the single nucleon sector, our result for neutral pion photoproduction on the deuteron is in agreement with experiment.

PACS number(s): 25.20.Lj, 12.39.Fe

I. INTRODUCTION

In recent times, there has been increasing interest in applying the method of chiral Lagrangians, or chiral perturbation theory (χPT), to processes involving more than a single nucleon [1–8]. This interest is motivated by the desire to determine what aspects of nuclear physics can be understood on the basis of the chiral symmetry of QCD. In the limit of vanishing u and d quark masses the QCD Lagrangian admits a global $SU(2)_L \times SU(2)_R$ chiral symmetry. The absence of parity doubling in the hadronic spectrum implies that this chiral symmetry is either anomalous or spontaneously broken by the QCD vacuum. The existence of suitable Goldstone boson candidates, the pions, bears out the latter conjecture. *A priori*, the space of chiral symmetric operators involving the relevant degrees of freedom — nucleons and pions — is infinite. Moreover, since the interactions are strong, nothing is really learned insofar as QCD is concerned by restricting oneself to any arbitrary finite subset of chiral symmetric operators, e.g., the simplest operators involving the fewest number of fields or renormalizable operators. Fortunately, as a consequence of nonlinearly realized chiral symmetry, low-energy hadronic matrix elements involving pions are analytic in momenta. The parameters that appear at leading order in small momenta are well known, and so chiral symmetry leads to nontrivial predictions at energies near the threshold of a physical process — so-called low-energy theorems (LET's). The crucial fact that the u and d quark masses are not identically zero can be straightforwardly accounted for in perturbation theory. As with any approximation scheme, the fundamental importance of χPT is its ability to handle corrections to the leading order in a systematic way [9]. This method has been applied with great success to the interactions of pions with a single nucleon [10,11]. One might then wonder what generic features of nuclear physics can be deduced from this chiral symmetry of QCD.

The main technical difficulty that arises when considering more than a single nucleon is that χPT necessarily breaks down, as is made clear by the appearance of shallow nuclear bound states [2]. This breakdown manifests itself via infrared singularities in Feynman diagrams evaluated in the static approximation. The problem is clear in the language of time-ordered perturbation theory. Evidently there are two types of energy denominators that can appear in a typical time-ordered graph. The first type arises from intermediate states which differ in energy from the initial and final states only by the emission or absorption of soft pions. These energy denominators are of the order of a small momentum or pion mass and are therefore consistent with the usual chiral power counting scheme. On the other hand, the second type of intermediate states differs in energy from the initial and final states by a nucleon three-momentum, and therefore blows up in the static limit. Graphs of the first type are called irreducible. Following the tenets of scattering theory, one can modify the rules and use χPT to calculate an effective potential, which consists of the sum of all N_n-nucleon irreducible graphs [1,2]. The S matrix, which of course includes all reducible contributions, is then obtained through iteration by solving a Lippmann-Schwinger equation. Several generic features of nuclear physics, including two- and few-body forces [2,4,5] and isospin violation [6], have been shown to arise naturally in this approach.

Here we will apply chiral perturbation theory to a scattering process involving light nuclei. This program was initiated several years ago by Weinberg [3], in a study of the pion-nucleus scattering lengths. The strategy is best described graphically. In Fig. 1 we display the anatomy of a scattering matrix element. χPT generates the irreducible kernel, which is then sewn to the external nuclear wave functions (with $N_n = A$). Nuclear wave functions, too, are calculable in χPT, and in fact exist for the deuteron [4]. A completely consistent calculation can be carried out, and results are reported here. However, this approach is in a sense counterproductive, since it is then unclear what aspect of chiral symmetry is being tested. In the spirit of χPT, where experimental input is always welcome, one should make use of the most successful phenomenological potential. This al-

*Electronic address: sbeane@phy.duke.edu
†Electronic address: clee@utpapa.ph.utexas.edu
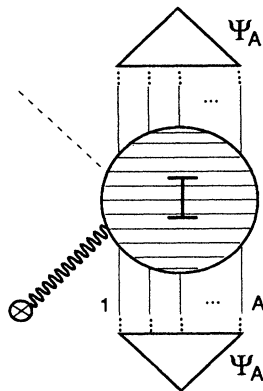‡Electronic address: vankolck@alpher.npl.washington.edu

FIG. 1. The anatomy of a matrix element. The Ψ_A's correspond to the nuclear wave functions. The blob is the sum of all A-nucleon irreducible graphs.

lows one to test the relevance of chiral symmetry in determining the irreducible scattering kernel. In the case of the deuteron, we also use the well-known Bonn potential wave function [12], which, although not respectful of chiral symmetry, is at least spiritually linked to QCD.

In this paper, we consider pion photoproduction on light nuclei at threshold. We carry out a general power counting analysis of photoproduction, but specialize to neutral pion photoproduction. We calculate a general formula for the invariant threshold amplitude to third order in small momenta. This process is of course interesting in its own right; there has been no systematic calculation based on chiral symmetry. Furthermore, as we will see, this process is intimately related to threshold neutral pion photoproduction on a single nucleon, a process which has caused a great deal of theoretical and experimental confusion. In contrast to pion-nucleus scattering at threshold [3], the amplitude for neutral pion photoproduction on nuclei, to third order in small momenta, has no undetermined parameters. Unfortunately, although the same is true in the single nucleon sector, evidently the amplitude there converges slowly at best. Hence the single-scattering contribution must be treated as phenomenological input. With a reasonable choice for this contribution, our result for the deuteron electric dipole amplitude is in agreement with experiment.

This paper is organized as follows. In Sec. II we review the standard power counting formulas. In Sec. III we present the heavy fermion effective Lagrangian to the order relevant to our calculation. Section IV consists of a power counting analysis of pion photoproduction on a nucleus composed of A nucleons. Here we give a general formula for the neutral pion photoproduction amplitude. We specialize to neutral pion photoproduction on the deuteron in Sec. V. Finally, we summarize and conclude. Several appendixes are included for pedagogical purposes.

II. POWER COUNTING

In the absence of exact solutions to quantum mechanical equations of motion, as in QCD, systematic statements are possible only when a small dimensionless expansion param-

eter is identified. One class of dimensionless parameters consists of pure numbers, such as a coupling constant associated with a renormalizable interaction, or the inverse of the dimensionality of a group, as in the large-$\mathcal{N}_c$ limit. A second class of dimensionless parameters consists of ratios of dimensional quantities. This class arises naturally via broken symmetries, and is the case of interest in this paper.

Spontaneously broken continuous symmetries give rise to massless Goldstone modes. These modes do not propagate in the vacuum, and therefore only couple derivatively. Hence at energies small relative to the characteristic symmetry breaking scale, the interactions of Goldstone bosons admit a power series in momenta. In QCD the small parameter is Q/Λ_χ, where Q is a characteristic momentum, and Λ_χ is the scale of chiral symmetry breaking —of order the masses of the lowest-lying resonances. The effects of nonzero quark masses give the pion a mass. Since M_π/Λ_χ is small, we treat Q as representing a small momentum or a pion mass. A generic matrix element involving the interaction of any number of pions and nucleons can then be written in the form

$$\mathcal{M} = Q^\nu \mathcal{F}(Q/\mu), \tag{1}$$

where μ is a renormalization scale, and ν is a counting index. It is straightforward to arrive at a general formula for ν by considering the momentum space structure of generic Feynman rules. In this way one finds [2]

$$\nu = 4L - I_n - 2I_\pi + \sum_i V_i d_i + 4 - 4C, \tag{2}$$

where L is the number of loops, $I_{n,\pi}$ is the number of internal fermion, pion lines, V_i is the number of vertices of type i, d_i is the number of derivatives or powers of M_π which contribute to an interaction of type i, and C is the number of separately connected pieces. One can also make use of the graph theoretic identities:

$$L = I_n + I_\pi - \sum_i V_i + 1, \tag{3}$$

$$2I_n + E_n = \sum_i V_i n_i, \tag{4}$$

where E_n is the number of external nucleon lines, and n_i is the number of fermion fields involved in an interaction of type i. Here we are interested in processes with the same number of nucleon lines in the initial and final state, and so defining $N_n \equiv E_n/2$, we obtain the master formula

$$\nu = 4 - N_n - 2C + 2L + \sum_i V_i \Delta_i, \tag{5}$$

$$\Delta_i \equiv d_i + n_i/2 - 2.$$

This formula is important because chiral symmetry places a lower bound $\Delta_i \geq 0$. Hence the leading irreducible graphs are tree graphs ($L = 0$) with the maximum number C of separately connected pieces, constructed from vertices with $\Delta_i = 0$.
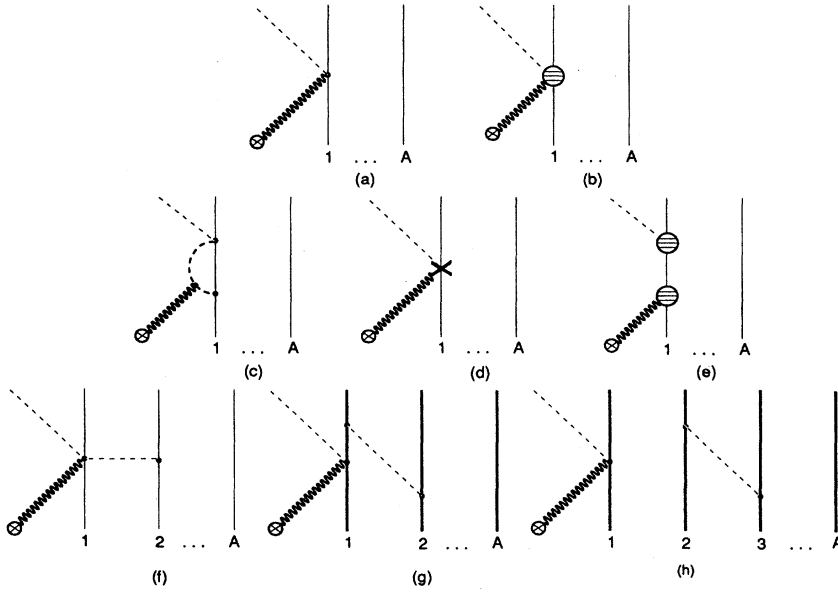
FIG. 2. Characteristic graphs which contribute at each order. The time-ordered graphs are distinguished by bold nucleon lines.

How is this analysis altered in the presence of an electromagnetic field? Photons couple via the electromagnetic field strength tensor and by minimal substitution. This has the simple effect of modifying the lower bound on Δ_i to $\Delta_i \geq -1$ (and, of course, of introducing an expansion in the electromagnetic coupling).

III. BARYON χPT

With the power counting scheme established, the next step is to construct the various interactions which contribute to matrix elements for a given value of ν. The technology that goes into building an effective Lagrangian is standard by now [10]. Here we establish our conventions. The pion triplet is contained in a matrix field

$$\Sigma = \exp\left(\frac{i\vec{\pi}\cdot\vec{\tau}}{f_\pi}\right), \tag{6}$$

which transforms under $SU(2)_L \times SU(2)_R$ as $\Sigma \to L\Sigma R^\dagger$. It is convenient to introduce the field $\xi \equiv \sqrt{\Sigma}$, with the transformation property $\xi \to L\xi U^\dagger = U\xi R^\dagger$. This transformation property implicitly defines U. Out of ξ one can construct

$$V_\mu = \frac{1}{2}[\xi^\dagger(\partial_\mu - ie\mathcal{A}_\mu Q)\xi + \xi(\partial_\mu - ie\mathcal{A}_\mu Q)\xi^\dagger], \tag{7}$$

$$A_\mu = \frac{i}{2}[\xi^\dagger(\partial_\mu - ie\mathcal{A}_\mu Q)\xi - \xi(\partial_\mu - ie\mathcal{A}_\mu Q)\xi^\dagger], \tag{8}$$

which transform as $V_\mu \to UV_\mu U^\dagger + U\partial_\mu U^\dagger$ and $A_\mu \to UA_\mu U^\dagger$ under $SU(2)_L \times SU(2)_R$. It is convenient to assign the nucleon doublet N the transformation property $N \to UN$. With these ingredients, one can construct the leading order effective Lagrangians

$$\mathcal{L}^{(2)}_{\pi\pi} = \frac{1}{4}f_\pi^2 \operatorname{tr}(D_\mu\Sigma^\dagger D^\mu\Sigma) + \frac{1}{4}f_\pi^2 M_\pi^2 \operatorname{tr}(\Sigma + \Sigma^\dagger), \tag{9}$$

$$\mathcal{L}^{(1)}_{\pi N} = i\bar{N}(\not{D} - m)N + g_A\bar{N}\not{A}\gamma_5 N, \tag{10}$$

$$\mathcal{L}^{(0)}_{NN} = \frac{1}{2}C_a(\bar{N}\Gamma_a N)^2, \tag{11}$$

where $D_\mu \equiv \partial_\mu + V_\mu$, Γ_a is an arbitrary Hermitian operator, and the C_a are undetermined coefficients. The pion covariant derivative is $D_\mu\Sigma = \partial_\mu\Sigma - ie\mathcal{A}_\mu[Q,\Sigma]$, where $Q = (1 + \tau_3)/2$. The appearance of the nucleon mass m, both explicitly and through the time derivative acting on the nucleon field, implies the existence of a dimensionless quantity that is
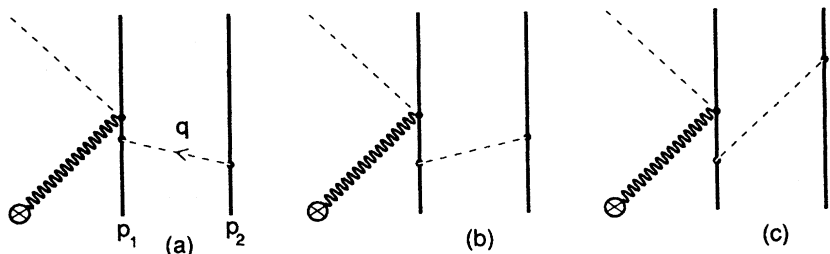
FIG. 3. The energy dependence of the impulse approximation graphs (a) and (b) approximately cancels the time-ordered three-body diagram (c).
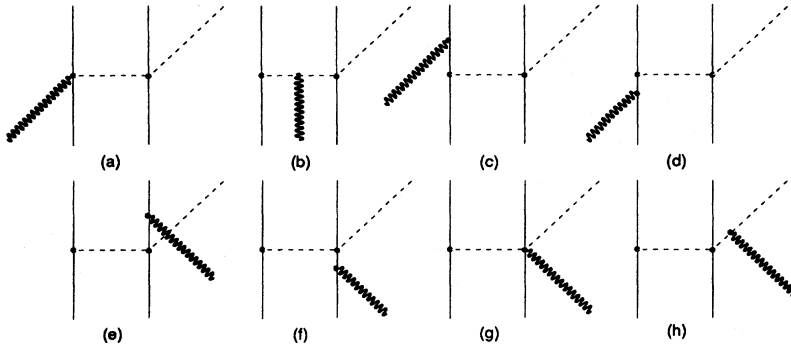
FIG. 4. Gauge-invariant subset of three-body interactions. In Coulomb gauge, only graphs (a) and (b) contribute to neutral pion photoproduction.

not small: $m/\Lambda_\chi \sim 1$. This destroys the power counting. Fortunately, since the nucleon carries a quantum number —baryon number— which is conserved by the strong interactions, one can maintain a consistent power counting framework by choosing a heavy-fermion basis in which the nucleon mass does not appear at leading order [13,14]. The nucleon momentum can be written as $p^\mu = mv^\mu + k^\mu$, where v^μ is the nucleon four-velocity ($v^2 = 1$), and k^μ is the amount by which the nucleon momentum is off shell. We can then define a velocity dependent basis

$$B_v(x) = e^{imv\cdot x}N(x).$$ (12)

In the rest frame of the nucleon, $v^\mu = (1,0,0,0)$. Although choosing a particular velocity breaks covariance, integrating over all velocity-dependent Lagrangians restores covariance [13]. The velocity-dependent Lagrangian in the new basis is

$$\mathscr{L}_v^{(1)} = i\bar{B}_v(v\cdot D)B_v + 2g_A\bar{B}_v(A\cdot S_v)B_v,$$ (13)

where S_v^μ is the spin operator. Note that the nucleon mass term is no longer present in the Lagrangian. The new effective expansion parameter is $|k|/\Lambda_\chi$. The $1/m$ corrections enter via higher dimensional operators which affect the higher orders in χPT. At next to leading order one finds

$$\mathscr{L}_v^{(2)} = \frac{1}{2m}\bar{B}_v(-D^2 + (v\cdot D)^2 + 2ig_A\{v\cdot A,S\cdot D\}$$

$$- \frac{i}{2}[S_v^\mu,S_v^\nu][(1+\kappa_v)f_{\mu\nu}^+$$

$$+ \tfrac{1}{2}(\kappa_s - \kappa_v)\mathrm{tr}f_{\mu\nu}^+] + \cdots)B_v,$$ (14)

where $\kappa_v = \kappa_p - \kappa_n$, $\kappa_s = \kappa_p + \kappa_n$, and $f_{\mu\nu}^+ \equiv e(\xi^\dagger Q\xi + \xi Q\xi^\dagger)F_{\mu\nu}$. $F_{\mu\nu}$ is the electromagnetic field strength tensor. The center dots signify that we have included only the interactions at this order which are relevant to our calculation. Note, finally, that the Δ isobar can be introduced in an analogous way.

IV. PION PHOTOPRODUCTION ON LIGHT NUCLEI

Now we can put our technology to use. Consider a process with $N_n = A$ nucleons in both the initial and final states, and a single photon and a single pion in the initial and final

states, respectively. Limiting ourselves to lowest order in the electromagnetic coupling, we can order the chiral expansion of the irreducible diagrams by way of the counting index ν.

A. $\nu=3-3A$

At leading order in small momenta, the matrix element is given by tree graphs with the maximum number of separately connected pieces ($L=0$, $C=A$) constructed out of one interaction with $\Delta_i = -1$, and interactions with $\Delta_i = 0$. For example, at this order one has the the Kroll-Ruderman term [Fig. 2(a)].

B. $\nu=4-3A$

The first corrections to the leading terms are still tree graphs with the maximum number of separately connected pieces ($L=0$, $C=A$), but have one vertex of higher index: (i) either one vertex with $\Delta_i = -1$ and one with $\Delta_i = 1$, (ii) or vertices with $\Delta_i = 0$, the one involving the photon field being a $1/m$ correction [Fig. 2(b)].

C. $\nu=5-3A$

There are four classes of corrections at this order.
(i) One-loop graphs ($L=1$) with interactions with $\Delta_i = -1,0$, and $C=A$ [Fig. 2(c)].
(ii) Counterterm graphs with $L=0$, $\Delta_i = 1$ and $C=A$ [Fig. 2(d)]. In the case of neutral pion photoproduction, these graphs vanish and only finite loop graphs remain.
(iii) $C=A$ tree ($L=0$) graphs with (i) $\Delta_i = -1,2$ interactions or (ii) $\Delta_i = 0,1$ interactions[1] [Fig. 2(e)] (some of these

---

[1]Note that there are no irreducible graphs of this type where the photon and the pion are attached to different nucleons, because energy and momentum conservation require an interaction between nucleons (for example, by pion exchange), and somewhere along the nucleon lines there is an energy flow of the order of the pion mass. The irreducible part of the diagram then contains the nucleon interaction, which decreases the number of separately connected pieces and renders the diagram higher order. At higher energies, where higher order contributions might become more important, it may well be necessary to account for such effects [15].

are $1/m^2$ corrections and are proportional to the nucleon magnetic moments).

(iv) Finally, there are tree graphs $(L=0)$ with one less than the maximum number of separately connected pieces $(C=A-1)$, and interactions with $\Delta_i=-1,0$. These graphs fall into two separate classes. There are the three-body graphs like the Feynman graph of Figs. 2(f) and the time-ordered graph of Fig. 2(g). For $A>2$, there are also disconnected two-body interactions as in Fig. 2(h).

In principle, all of these graphs contribute to pion photo-

production on nuclei. However, some generic simplifications arise when one sews in the nuclear wavefunctions.

First, the time-ordered graphs of type 2(g) and 2(h) get canceled against recoil in the one-pion-exchange piece of the potential. In order to see this, consider the three diagrams of Fig. 3. These graphs all have the same spin-isospin structure: They differ only in the energy denominators. The first two graphs [Figs. 3(a) and 3(b)] arise when a diagram like 2(a) is sandwiched between wave functions obtained from a potential whose long range part comes from pion exchange. They are proportional to

$$\frac{1}{E(\vec{p}_1-\vec{q})+E(\vec{p}_2+\vec{q})-E(\vec{p}_1)-E(\vec{p}_2)}\left[\frac{1}{E(\vec{p}_1-\vec{q})+w-E(\vec{p}_1)}+\frac{1}{E(\vec{p}_2+\vec{q})+w-E(\vec{p}_2)}\right]$$

$$=\frac{2}{w[E(\vec{p}_1-\vec{q})+E(\vec{p}_2+\vec{q})-E(\vec{p}_1)-E(\vec{p}_2)]}-\frac{1}{w^2}\left[1+O\left(\frac{E}{w}\right)\right]. \quad (15)$$

The first term corresponds to static one-pion exchange in the potential; it is big, as anticipated, because these reducible diagrams have small nucleon energy denominators. The second term is smaller because of the additional small recoil numerator, while the dots sum higher orders in chiral perturbation theory. On the other hand, the remaining graph [Fig. 3(c)] is proportional to

$$\frac{1}{w^2}\left[1+O\left(\frac{E}{w}\right)\right], \quad (16)$$

and exactly cancels recoil in the reducible diagrams. Similar cancellations can be found among the other time-ordered diagrams. In other words, to this order in chiral perturbation theory we can omit the time-ordered diagrams 2(g) and 2(h) by at the same time disregarding the energy dependence in the potential.

Second, in the case of neutral pion photoproduction at threshold a number of the graphs in Fig. 2 will not contribute: those where the photon line is attached to a pion and those that go like $S\cdot q$, where q is the outgoing pion momentum. In particular, all the leading order graphs vanish [Fig. 2(a)], which immediately suggests that the cross section will be smaller than for charged pion production, and — of particular interest to us — more sensitive to two-nucleon contributions. Moreover, the three-body time-ordered graphs [Fig. 2(g)] and the two-body disconnected graphs [Fig. 2(h)] also vanish, and so we can expect little influence of the energy-dependent part of the potential. As noted above, the loop graphs are finite for a neutral pion, and so there are no undetermined parameters to this order.

Since all single-scattering contributions have been calculated to third order in small momenta, all that is left to calculate are the three-body graphs of Fig. 4. In Coulomb gauge $(v\cdot\epsilon=0)$, only Figs. 4(a) and 4(b) survive. Hence, to $\vartheta(q^3)$ in χPT, the threshold amplitude for neutral pion photoproduction on a nucleus is remarkably simple. We obtain the general formula

$$\mathcal{M}_{\Psi_A}|_{q=0}=\mathcal{M}_{\Psi_A}^{ss}+\mathcal{M}_{\Psi_A}^{(a)}+\mathcal{M}_{\Psi_A}^{(b)}, \quad (17)$$

where

$$\mathcal{M}_{\Psi_A}^{ss}=S_{\Psi_A}(k)\sum_i\mathcal{M}_N^i, \quad (18)$$

$$\mathcal{M}_{\Psi_A}^{(a)}=i\frac{2eg_AM_\pi m}{(2\pi)^3f_\pi^3}$$
$$\times\sum_{i<j}\left\langle\Psi_A\left|(\vec{\tau}^{(i)}\cdot\vec{\tau}^{(j)}-\tau_z^{(i)}\tau_z^{(j)})\frac{(\vec{J}\cdot\vec{\epsilon})}{\vec{q}_{ij}'^2}\right|\Psi_A\right\rangle, \quad (19)$$

$$\mathcal{M}_{\Psi_A}^{(b)}=i\frac{4eg_AM_\pi m}{(2\pi)^3f_\pi^3}$$
$$\times\sum_{i<j}\left\langle\Psi_A\left|(\vec{\tau}^{(i)}\cdot\vec{\tau}^{(j)}-\tau_z^{(i)}\tau_z^{(j)})\right.\right.$$
$$\times\left.\left.\frac{[\vec{J}\cdot(\vec{q}_{ij}'-\vec{k})](\vec{q}_{ij}'\cdot\vec{\epsilon})}{[(\vec{q}_{ij}'-\vec{k})^2+M_\pi^2]\vec{q}_{ij}'^2}\right|\Psi_A\right\rangle. \quad (20)$$

$S_{\Psi_A}(k)$ is a generic overlap function. (See next section and appendixes for details.)

The single-scattering electric dipole amplitudes have been calculated to $\vartheta(q^3)$ without an explicit isobar field, and are given by [16]

$$E_{0+}^{\pi^0p}=-\frac{eg_A}{8\pi f_\pi}\left\{\frac{M_\pi}{m}-\frac{M_\pi^2}{2m^2}(3+\kappa_p)-\frac{M_\pi^2}{16f_\pi^2}\right\},$$

$$E_{0+}^{\pi^0n}=-\frac{eg_A}{8\pi f_\pi}\left\{\frac{M_\pi^2}{2m^2}\kappa_n-\frac{M_\pi^2}{16f_\pi^2}\right\}. \quad (21)$$

Unfortunately, the single-nucleon sector is not well understood. On the one hand, the neutron amplitude has not been

measured. On the other hand, the electric dipole amplitude $E_{0+}^{\pi^0 p}$ has an interesting — and rather complicated — history, which we will briefly discuss here.[2] An expansion of the amplitude in powers of the pion energy was first used to derive a tree level "LET" [18] yielding a value $E_{0+}^{\pi^0 p} = -2.23 \times 10^{-3}/M_{\pi^+}$; this LET was later rederived [19] under an extended partially conserved axial vector current (PCAC) hypothesis, in a way that made explicit that it also included loop corrections, like rescattering. Experiments at Mainz [20] and Saclay [21] suggested a violation of this LET. Subsequently, the data were reexamined, leading to the revised value $E_{0+}^{\pi^0 p} = (-2.0 \pm 0.2) \times 10^{-3}/M_{\pi^+}$, a result in agreement with the "classical" LET [22]. The source of the discrepancy is isospin violation; the difference of 6.8 MeV between the $p\pi^0$ and $n\pi^+$ threshold leads to a rapid variation of the amplitude in this region. The correct interpretation of the data depends critically on the details of this variation. The situation as of 1991 is reviewed in [22]. To further complicate the matter, it was then found that there are additional *large* finite loop contributions to $E_{0+}^{\pi^0 p}$ at $\vartheta(q^3)$, the so-called triangle graphs [see Fig. 2(c)] [16,23,24]. They are of higher order in the expansion in pion energy, but are proportional to M_π^{-1} [16,25]. With these contributions — which clearly must be included — the $\vartheta(q^3)$ LET no longer seems to agree with the data. Moreover, it is clear that $E_{0+}^{\pi^0 p}$ is — at best — slowly converging. $E_{0+}^{\pi^0 p}$ has now been calculated to $\vartheta(q^4)$, and shows no signs of converging. Evidently, it is difficult to escape the conclusion that the s-wave multipole is not a good testing ground of QCD. All is not lost, however; recently novel p-wave LET's have been calculated, and found to have better convergence properties than the s waves [26]. Nevertheless, this failure of χPT in describing the s waves without explicit isobar fields is a lesson that cannot be ignored here. Evidently the sensible thing to do is to make a best phenomenological estimate of the single-scattering contribution. The chiral prediction without the triangle graphs would appear to be a reasonable phenomenological estimate of $E_{0+}^{\pi^0 p}$, and so we assume the same for $E_{0+}^{\pi^0 n}$.

V. NEUTRAL PION PHOTOPRODUCTION ON THE DEUTERON

Here we will consider the deuteron. Deuteron phase shifts and properties are well described by the Bonn wave function [12]. We also give — in parentheses — the chiral wave function [4] results. With the conventions defined in the appendixes, the single-scattering contribution to the deuteron is given by

$$E_d^{ss} = \frac{1 + M_\pi/m}{1 + M_\pi/m_d}(E_{0+}^{\pi^0 p} + E_{0+}^{\pi^0 n})S_d(k/2)$$

$$= -1.34 \times 10^{-3}/M_{\pi^+} \quad (-1.38), \qquad (22)$$

where $S_d(k/2)$ is the deuteron form factor,

---

[2]For a review, see [17].

$$S_d(k/2) = \int d^3 p\, \phi_f^*(p)\phi_i\left(p - \frac{k}{2}\right) = 0.722 \quad (0.742),$$

$$\qquad (23)$$

evaluated with the Bonn and chiral wave functions, respectively, and we have used the phenomenological estimates

$$E_{0+}^{\pi^0 p} = -\frac{eg_A}{8\pi f_\pi}\left\{\frac{M_\pi}{m} - \frac{M_\pi^2}{2m^2}(3 + \kappa_p)\right\}$$

$$= -2.24 \times 10^{-3}/M_{\pi^+},$$

$$E_{0+}^{\pi^0 n} = -\frac{eg_A}{8\pi f_\pi}\left\{\frac{M_\pi^2}{2m^2}\kappa_n\right\} = 0.5 \times 10^{-3}/M_{\pi^+}. \qquad (24)$$

[The corresponding result from the "complete" $\vartheta(q^3)$, Eq. (21), will also be discussed shortly.] The three-body contributions are readily obtained (see appendixes for details). Figure 4(a) yields

$$E_d^{(a)} = -\frac{eg_A M_\pi m}{8\pi(M_\pi + m_d)\pi f_\pi^3 k}\int_0^\infty \frac{U^2}{r^2}\sin\left(\frac{kr}{2}\right)dr$$

$$= -2.20 \times 10^{-3}/M_{\pi^+} \quad (-2.18), \qquad (25)$$

and Fig. 4(b) yields

$$E_d^{(b)} = -\frac{eg_A M_\pi m}{8\pi(M_\pi + m_d)2\pi f_\pi^3}\int_0^1 dz \int_0^\infty dr\, e^{-m'r}U^2$$

$$\times \left[\frac{1}{r}\frac{\sin[(z - \frac{1}{2})kr]}{(z - \frac{1}{2})kr} - \left(\frac{1}{r} + m'\right)\right.$$

$$\times \left.\left\{\frac{\sin(z - \frac{1}{2})kr}{[(z - \frac{1}{2})kr]^3} - \frac{\cos(z - \frac{1}{2})kr}{[(z - \frac{1}{2})kr]^2}\right\}\right]$$

$$= -0.43 \times 10^{-3}/M_{\pi^+} \quad (-0.39). \qquad (26)$$

The total is then given by

$$E_d = E_d^{ss} + E_d^{(a)} + E_d^{(b)} = -3.97 \times 10^{-3}/M_{\pi^+} \quad (-3.95), \qquad (27)$$

to be compared to the experimental value [27]

$$E_d^{expt} = (-3.74 \pm 0.25) \times 10^{-3}/M_{\pi^+}. \qquad (28)$$

Hence the simple picture provided by chiral symmetry does fairly well. In particular, the importance of the three-body correction (charge exchange contribution) emerges as a consequence of chiral symmetry. It is gratifying that the results are not particularly sensitive to the details of the wave function. There are of course several serious caveats. Strictly speaking the $\vartheta(q^3)$ result without explicit isobars fairs badly, as is made clear in Table I. This is, of course, a consequence of the theoretical failure in the single-nucleon sector. Better experimental data is necessary in the single-scattering sector. Currently new measurements of $E_{0+}^{\pi^0 p}$ are underway at Mainz and Saskatoon [11]. In principle, with an accurate measurement of the deuteron photoproduction amplitude one could extract the neutron electric dipole ampli-

TABLE I. The importance of the single-scattering contribution: The χPT predictions at $\vartheta(q^3)$ without the triangle graphs — serving as a phenomenological estimate — lead to agreement with the experimental value of E_d [27].

	$E_{0+}^{\pi^0 p}$	$E_{0+}^{\pi^0 n}$	E_d^{ss}	E_d
$\vartheta(q^3)$ incomplete	-2.24	0.5	-1.33	-3.97
$\vartheta(q^3)$	0.96	3.7	3.6	0.94
Experiment	-2.0±0.2 (?)	?	-	-3.74±0.25

tude using our results. Of course, in order to be convinced of the soundness of this method one would have to calculate $\vartheta(q^4)$ three-body effects in order to test the convergence properties of the nuclear matrix elements. Finally, we note that our final results are quite similar to results obtained some time ago, based on the photoproduction low-energy theorems in the impulse approximation, and assorted estimates of the three-body corrections [28–30]. One might say that we have placed these successful results on a more sound theoretical footing by determining — by way of chiral power counting — the precise graphs that should dominate at threshold.

VI. CONCLUSION

We have taken a pedagogical approach to pion photoproduction on nuclei in the framework of baryon chiral perturbation theory. The method presented allows one to make systematic use of chiral symmetry in a scattering process involving nuclei. In general, calculations are more involved than those of the single-nucleon sector, since one must focus on the set of irreducible graphs, which requires use of time-ordered perturbation theory. In the special case of neutral pion photoproduction, the amplitude to $\vartheta(q^3)$ is simple, involving only tree level Feynman graphs evaluated in the heavy-fermion formalism. We evaluated the deuteron electric dipole amplitude using the Bonn and chiral wave functions, together with a phenomenological estimate for the single-nucleon (impulse approximation) contributions. The result of this calculation, like that of the π-deuteron scattering length [3], is in agreement with experiment. Hence the importance of three-body contributions emerges in both cases as a consequence of chiral symmetry. The result is, of course, critically dependent on input from the single-nucleon sector. Therefore, a more accurate determination of the nucleon electric dipole amplitudes is clearly required in order to make definite predictions for nuclei. There are many other processes which can be explored using this technology. Charged pion photoproduction is of great interest since in that case the single-nucleon sector is well understood both theoretically and experimentally. Also, results — both scattering lengths and photoproduction amplitudes — for heavier nuclei like tritium or helium would be a particularly novel way to explore the relevance of chiral symmetry in nuclei.

ACKNOWLEDGMENTS

APPENDIX A: NORMALIZATION CONVENTIONS

With field normalization convention, the differential cross section for $\gamma d \to \pi d$ can be written as

$$d\sigma = \frac{(2\pi)^4}{u_\alpha} \delta^4(p_1 + k - p_2 - q)$$

$$\times \frac{\overline{|\mathcal{M}|^2}}{2E_1 \, 2E_2 \, 2\omega_q \, 2\omega_k} \frac{d^3\vec{p}_2}{(2\pi)^3} \frac{d^3\vec{q}}{(2\pi)^3}, \quad (A1)$$

where p_1, p_2 are the momenta of the initial and final deuterons, and q,k are the momenta of the outcoming neutral pion and photon, respectively. u_α is the relative velocity of the incident particles, given by

$$u_\alpha = \frac{p_1 \cdot k}{E_1 \omega_k}. \quad (A2)$$

In the center-of-mass frame one finds

$$d\sigma = \frac{1}{64\pi^2 u_\alpha} \frac{\overline{|\mathcal{M}|^2}}{E_1 E_2 \omega_q \omega_k} \delta(E_1 + \omega_k - E_2 - \omega_q) q^2 dq d\Omega. \quad (A3)$$

The integration over q readily yields

$$d\sigma = \frac{1}{64\pi^2} \frac{E_1}{E_1 + |\vec{k}|} \frac{\overline{|\mathcal{M}|^2}}{E_1 E_2 \omega_q \omega_k} q^2 \frac{E_2 \omega_q}{q(E_2 + \omega_q)} d\Omega$$

$$= \frac{1}{64\pi^2} \frac{q}{|\vec{k}|} \frac{\overline{|\mathcal{M}|^2}}{(E_1 + |\vec{k}|)(E_2 + \omega_q)} d\Omega, \quad (A4)$$

where $\omega_k = k$, and E_1, E_2, and ω_q are the energies of the deuterons and the pion, respectively. The slope of the differential cross section at threshold is defined as

$$\frac{|\vec{k}|}{q} \frac{d\sigma}{d\Omega}\bigg|_{q=0} = \frac{1}{64\pi^2} \frac{\overline{|\mathcal{M}|^2}_{q=0}}{(\sqrt{m_d^2 + M_\pi^2} + |\vec{k}|)(m_d + M_\pi)}$$

$$\approx \frac{1}{64\pi^2} \frac{\overline{|\mathcal{M}|^2}_{q=0}}{(m_d + M_\pi)^2}. \quad (A5)$$

We can express the photoproduction amplitude in terms of rotationally invariant amplitudes:

$$\mathcal{M} = i\vec{J} \cdot \vec{a} \mathcal{M}_1 + i\vec{J} \cdot \vec{k}\vec{q} \cdot \vec{a} \mathcal{M}_2 + i\vec{J} \cdot \vec{q}\vec{q} \cdot \vec{a} \mathcal{M}_3$$

$$+ i\vec{q} \cdot \vec{k}\vec{a} \mathcal{M}_4, \quad (A6)$$

where $\vec{a} \equiv \vec{\epsilon} - (\vec{k} \cdot \vec{\epsilon})\vec{\epsilon}$. It is convenient to define an electric dipole amplitude E_d such that, in Coulomb gauge,

$$\mathcal{M}|_{q=0} = \mathcal{M}_d \equiv 8\pi(m_d + M_\pi) \, 2i(\vec{\epsilon} \cdot \vec{J})E_d, \quad (A7)$$

where $\vec{J} = \frac{1}{2}(\vec{\sigma}_n + \vec{\sigma}_p)$. It then follows that

$$\frac{|\vec{k}|}{q}\frac{d\sigma}{d\Omega}\Big|_{q=0} = \frac{8}{3}E_d^2. \tag{A8}$$

APPENDIX B: THE S MATRIX

The S matrix is defined as

$$S_{fi} = -i(2\pi)^4 \delta^4(p_i - p_f)\left(\prod_{i=1}^{n}\frac{1}{\sqrt{(2\pi)^3 2E_i}}\right)\mathcal{M}, \tag{B1}$$

where n is the total number of external particles. For the three-body process $\gamma NN \to \pi NN$, we find

$$S_{fi} = -i(2\pi)^4 \delta^4(p_i - p_f)$$
$$\times \frac{\mathcal{M}_{NN}}{(2\pi)^9\sqrt{2E_1\,2E_2\,2E_1'\,2E_2'\,2E_\gamma\,2E_\pi}}, \tag{B2}$$

whereas the S-matrix for $\gamma d \to \pi d$ is given by

$$S_{fi} = -i(2\pi)^4 \delta^4(p_i - p_f)\frac{\mathcal{M}_d}{(2\pi)^6\sqrt{2E_d\,2E_d'\,2E_\gamma\,2E_\pi}}. \tag{B3}$$

Therefore,

$$\mathcal{M}_d = \frac{1}{(2\pi)^3}\sqrt{\frac{E_d E_d'}{4\,E_1 E_2 E_1' E_2'}}\,\mathcal{M}_{NN}. \tag{B4}$$

Near threshold,

$$E_d \approx \sqrt{m_d^2 + \vec{k}^2} \approx m_d, \quad E_d' \approx m_d, \quad E_1 = E_2 = E_1' = E_2' \approx m, \tag{B5}$$

and so we obtain

$$\mathcal{M}_d = \frac{1}{(2\pi)^3 m}\mathcal{M}_{NN}. \tag{B6}$$

APPENDIX C: FEYNMAN AMPLITUDES

First we need the transition operator for $\gamma NN \to \pi NN$. Figure 4(a) yields

$$iT_{NN}^{(a)} = \bar{B}_{v_1}\left(\frac{ieg_A}{f_\pi}S_{v_1}^\mu \epsilon_{a3c}\tau_c^1 \epsilon_\mu\right)B_{v_1}\frac{i}{q'^2 - M_\pi^2}$$
$$\times \bar{B}_{v_2}\left(\frac{(q'+q)_\nu v_2^\nu}{4f_\pi^2}\epsilon_{a3d}\tau_d^2\right)B_{v_2} + (1 \leftrightarrow 2)$$
$$= -\frac{eg_A}{4f_\pi^3}\bar{B}_{v_1}S_{v_1}^\mu B_{v_1}\epsilon_\mu\frac{(q'+q)\cdot v_2}{q'^2 - M_\pi^2}\bar{B}_{v_2}B_{v_2}$$
$$\times \epsilon_{a3c}\epsilon_{a3d}\tau_c^1\tau_d^2 + (1 \leftrightarrow 2), \tag{C1}$$

where $\vec{q}' = \vec{p} - \vec{p}'$. We can make use of the relation

$$\bar{B}_v S_v^\mu B_v \approx 2m(\tfrac{1}{2}\vec{\sigma}\cdot\vec{v}, \tfrac{1}{2}\vec{\sigma}) \tag{C2}$$

to obtain

$$iT_{NN}^{(a)} = -\frac{eg_A}{4f_\pi^3}(2m)^2\frac{1}{2}\vec{\sigma}_1\cdot\vec{\epsilon}\frac{2M_\pi}{\vec{q}'^2}(\vec{\tau}^1\cdot\vec{\tau}^2 - \tau_z^1\tau_z^2) + (1 \leftrightarrow 2). \tag{C3}$$

Here we approximated $q_0 \approx q_0' \approx M_\pi$ and chose the Coulomb gauge ($\epsilon_0 = 0$ and $\vec{\epsilon}\cdot\vec{k} = 0$). Using the relation between the transition operator of $\gamma NN \to \pi NN$ and $\gamma d \to \pi d$, obtained in Appendix B, we get

$$iT_d^{(a)} = -\frac{2eg_A M_\pi m}{(2\pi)^3 f_\pi^3}\frac{\vec{J}\cdot\vec{\epsilon}}{(\vec{p}-\vec{p}')^2}(\vec{\tau}^1\cdot\vec{\tau}^2 - \tau_z^1\tau_z^2). \tag{C4}$$

The contribution from Fig. 4(b) is

$$iT_{NN}^{(b)} = \bar{B}_{v_1}\left(-\frac{g_A}{f_\pi}S_{v_1}^\mu q_\mu''\tau_a^1\right)B_{v_1}\frac{i}{q''^2 - M_\pi^2}e\,\epsilon_{a3c}(q''+q')^\mu\epsilon_\mu$$
$$\times \frac{i}{q'^2 - M_\pi^2}\bar{B}_{v_2}\left(\frac{1}{4f_\pi^2}(q'+q)_\nu v_2^\nu\epsilon_{c3b}\tau_b^2\right)B_{v_2} + (1 \leftrightarrow 2)$$
$$= \frac{eg_A}{4f_\pi^3}(2m)^2\,2M_\pi(\tfrac{1}{2}\vec{\sigma}_1\cdot\vec{q}'')\frac{2\vec{q}'\cdot\vec{\epsilon}}{(\vec{q}''^2 + M_\pi^2)\vec{q}'^2}(-)\epsilon_{c3a}$$
$$\times \epsilon_{c3b}\tau_a^1\tau_b^2 + (1 \leftrightarrow 2)$$
$$= -\frac{eg_A}{4f_\pi^3}(2m)^2\,2M_\pi(\vec{J}\cdot\vec{q}'')\frac{2\vec{q}'\cdot\vec{\epsilon}}{(\vec{q}''^2 + M_\pi^2)\vec{q}'^2}$$
$$\times (\vec{\tau}^1\cdot\vec{\tau}^2 - \tau_z^1\tau_z^2). \tag{C5}$$

It then follows that

$$iT_d^{(b)} = -\frac{2eg_A M_\pi m}{(2\pi)^3 f_\pi^3}\frac{2(\vec{J}\cdot\vec{q}'')\vec{q}'\cdot\vec{\epsilon}}{(\vec{q}''^2 + M_\pi^2)\vec{q}'^2}(\vec{\tau}^1\cdot\vec{\tau}^2 - \tau_z^1\tau_z^2), \tag{C6}$$

where $\vec{q}'' = \vec{p} - \vec{p}' - \vec{k}$. By sandwiching these transition operators between initial and final states, which include the effect of the nuclear wave functions, we obtain the total matrix element

$$\mathcal{M}_d = \langle f|T_d|i\rangle. \tag{C7}$$

Finally, we obtain

$$\mathcal{M}_d^{(a)} = i\frac{2eg_A M_\pi m}{(2\pi)^3 f_\pi^3}\left\langle \Psi_d\left|(\vec{\tau}^1\cdot\vec{\tau}^2 - \tau_z^1\tau_z^2)\frac{\vec{J}\cdot\vec{\epsilon}}{\vec{q}'^2}\right|\Psi_d\right\rangle, \tag{C8}$$

$$\mathcal{M}_d^{(b)} = i\frac{4eg_A M_\pi m}{(2\pi)^3 f_\pi^3}\left\langle \Psi_d\left|(\vec{\tau}^1\cdot\vec{\tau}^2 - \tau_z^1\tau_z^2)\right.\right.$$
$$\times \left.\left.\frac{(\vec{J}\cdot\vec{q}'')\vec{q}'\cdot\vec{\epsilon}}{(\vec{q}''^2 + M_\pi^2)\vec{q}'^2}\right|\Psi_d\right\rangle. \tag{C9}$$

It is straightforward to check that $\langle\vec{\tau}^1\cdot\vec{\tau}^2 - \tau_z^1\tau_z^2\rangle = -2$.

APPENDIX D: NUCLEAR MATRIX ELEMENTS

In this appendix we obtain the coordinate space representation of our matrix elements and evaluate using the Bonn potential. Consider first the momentum-dependent part of $\mathscr{M}_d^{(a)}$:

$$\left\langle \frac{\vec{J}\cdot\vec{\epsilon}}{(\vec{p}-\vec{p'})^2} \right\rangle$$

$$= \int d^3\vec{p}\, d^3\vec{p'}\, \tilde{\phi}_f^*(\vec{p'}) \frac{\vec{J}\cdot\vec{\epsilon}}{(\vec{p}-\vec{p'})^2} \tilde{\phi}_i\left(\vec{p}-\frac{\vec{k}}{2}\right)$$

$$= \frac{1}{4\pi} \int d^3\vec{r}\, d^3\vec{p}\, d^3\vec{p'}\, \tilde{\phi}_f^*(\vec{p'})$$

$$\times (\vec{J}\cdot\vec{\epsilon}) \frac{e^{-i(\vec{p}-\vec{p'})\cdot\vec{r}}}{r} \tilde{\phi}_i\left(\vec{p}-\frac{\vec{k}}{2}\right)$$

$$= \frac{(2\pi)^3}{4\pi} \int d^3\vec{r}\left(\frac{1}{(2\pi)^{3/2}} \int d^3\vec{p'}\, e^{i\vec{p'}\cdot\vec{r}}\, \tilde{\phi}_f^*(\vec{p'}) \right)$$

$$\times (\vec{J}\cdot\vec{\epsilon}) \frac{e^{-i\frac{\vec{k}}{2}\cdot\vec{r}}}{r}\left[\frac{1}{(2\pi)^{3/2}} \int d^3\vec{p}\exp\left[-i\left(\vec{p}-\frac{\vec{k}}{2}\right)\cdot\vec{r}\right] \right.$$

$$\left. \times \tilde{\phi}_i\left(\vec{p}-\frac{\vec{k}}{2}\right)\right]$$

$$= 2\pi^2 \int d^3\vec{r}\, \phi_f^*(\vec{r})(\vec{J}\cdot\vec{\epsilon}) \frac{\exp\left(-i\frac{\vec{k}}{2}\cdot\vec{r}\right)}{r} \phi_i(\vec{r}), \qquad \text{(D1)}$$

where ϕ is the spatial part of the deuteron wave function, and the identity

$$\frac{1}{\vec{q}^2} = \frac{1}{4\pi} \int d^3\vec{r}\, \frac{e^{i\vec{q}\cdot\vec{r}}}{r} \qquad \text{(D2)}$$

has been used. The spatial part of the deuteron wave function is

$$\phi(\vec{r}) = \frac{1}{\sqrt{4\pi}}\left(\frac{U(r)}{r} + \frac{1}{\sqrt{8}} S_{12}(\hat{r})\frac{W(r)}{r} \right), \qquad \text{(D3)}$$

where $U(r)$ and $W(r)$ are the S state and the D state of the radial wave function, respectively, normalized such that $\int_0^\infty dr(U^2+W^2) = 1$. The spin operator is defined to be

$$S_{12}(\hat{r}) = 3(\vec{\sigma}_1\cdot\hat{r})(\vec{\sigma}_2\cdot\hat{r}) - \vec{\sigma}_1\cdot\vec{\sigma}_2. \qquad \text{(D4)}$$

Since the S-state wave function has no angular dependence, the contribution from the S state is easily evaluated:

$$\left\langle \frac{\vec{J}\cdot\vec{\epsilon}}{(\vec{p}-\vec{p'})^2} \right\rangle_{S\text{ state}} = \frac{\pi}{2}(\vec{J}\cdot\vec{\epsilon})\int d^3\vec{r}\frac{U^2}{r^3}\exp\left(-i\frac{\vec{k}}{2}\cdot\vec{r}\right)$$

$$= \pi^2(\vec{J}\cdot\vec{\epsilon})\int_0^\infty \frac{U^2}{r}dr \int_{-1}^1 dx$$

$$\times \exp\left(-i\frac{kr}{2}x\right)$$

$$= \frac{4\pi^2}{k}(\vec{J}\cdot\vec{\epsilon})\int_0^\infty \frac{U^2}{r^2}\sin\left(\frac{kr}{2}\right)dr. \qquad \text{(D5)}$$

Next, we consider the effect of the D-state part of the wave function, which consists of the cross term as well as the pure D component. The cross term is given by

$$\left\langle \frac{\vec{J}\cdot\vec{\epsilon}}{(\vec{p}-\vec{p'})^2} \right\rangle_{\text{cross}} = \frac{\pi}{2\sqrt{8}}\int_0^\infty dr \frac{UW}{r}$$

$$\times \int d\Omega\exp\left(-i\frac{\vec{k}}{2}\cdot\vec{r}\right)\{\vec{J}\cdot\vec{\epsilon}S_{12}(\hat{r})$$

$$+ S_{12}(\hat{r})\vec{J}\cdot\vec{\epsilon}\}. \qquad \text{(D6)}$$

Here we can use $\{\vec{\sigma}_i,\vec{\sigma}_j\} = 2\delta_{ij}$ to show that

$$\vec{J}\cdot\vec{\epsilon}S_{12}(\hat{r}) + S_{12}(\hat{r})\vec{J}\cdot\vec{\epsilon} = 6(\vec{\epsilon}\cdot\hat{r})(\vec{J}\cdot\hat{r}) - 2(\vec{J}\cdot\vec{\epsilon}), \qquad \text{(D7)}$$

and the cross term becomes

$$\left\langle \frac{\vec{J}\cdot\vec{\epsilon}}{(\vec{p}-\vec{p'})^2} \right\rangle_{\text{cross}} = \frac{\pi}{\sqrt{8}}\int_0^\infty dr \frac{UW}{r}$$

$$\times \int d\Omega\exp\left(-i\frac{\vec{k}}{2}\cdot\vec{r}\right)\{3(\vec{\epsilon}\cdot\hat{r})(\vec{J}\cdot\hat{r})$$

$$- (\vec{J}\cdot\vec{\epsilon})\}. \qquad \text{(D8)}$$

The angular integration yields

$$\int d\Omega\exp\left(-i\frac{\vec{k}}{2}\cdot\vec{r}\right)(\vec{\epsilon}\cdot\hat{r})(\vec{J}\cdot\hat{r})$$

$$= (\vec{J}\cdot\vec{\epsilon})\frac{4\pi}{a^3}(\sin a - a\cos a), \qquad \text{(D9)}$$

where $a = kr/2$. Finally we have

$$\left\langle \frac{\vec{J}\cdot\vec{\epsilon}}{(\vec{p}-\vec{p'})^2} \right\rangle_{\text{cross}} = \frac{8\pi^2\sqrt{2}}{k^3}(\vec{J}\cdot\vec{\epsilon})\int_0^\infty dr \frac{UW}{r^4}$$

$$\times \left\{ 3\sin\frac{kr}{2} - 3\frac{kr}{2}\cos\frac{kr}{2} - \left(\frac{kr}{2}\right)^2\sin\frac{kr}{2} \right\}. \qquad \text{(D10)}$$

The pure D-state contribution can be evaluated in similar fashion:

$$\left\langle \frac{\vec{J}\cdot\vec{\epsilon}}{(\vec{p}-\vec{p}')^2} \right\rangle_{D \text{ state}}$$

$$= \frac{\pi}{16}\int dr \frac{W^2}{r}\int d\Omega \exp\left(-i\frac{\vec{k}}{2}\cdot\vec{r}\right)S_{12}^*(\vec{J}\cdot\vec{\epsilon})S_{12}$$

$$= \frac{\pi}{16}\int dr \frac{W^2}{r}\int d\Omega \exp\left(-i\frac{\vec{k}}{2}\cdot\vec{r}\right)6[2(\vec{\epsilon}\cdot\hat{r})(\vec{J}\cdot\vec{\epsilon})$$

$$-(\vec{J}\cdot\vec{\epsilon})]$$

$$= \frac{3\pi^2}{k^3}(\vec{J}\cdot\vec{\epsilon})\int dr \frac{W^2}{r^4}\left(8 \sin\frac{kr}{2}-4 \cos\frac{kr}{2}-\sin\frac{kr}{2}\right).$$

$$\text{(D11)}$$

Evaluating the integrals with the Bonn potential yields

$$\left\langle \frac{\vec{J}\cdot\vec{\epsilon}}{(\vec{p}-\vec{p}')^2} \right\rangle_{S \text{ state}} = (\vec{J}\cdot\vec{\epsilon})\ 7.616\ \text{fm}^{-1},$$

$$\left\langle \frac{\vec{J}\cdot\vec{\epsilon}}{(\vec{p}-\vec{p}')^2} \right\rangle_{\text{cross}} = (\vec{J}\cdot\vec{\epsilon})\ 0.051\ \text{fm}^{-1},$$

$$\left\langle \frac{\vec{J}\cdot\vec{\epsilon}}{(\vec{p}-\vec{p}')^2} \right\rangle_{D \text{ state}} = (\vec{J}\cdot\vec{\epsilon})(-0.090)\ \text{fm}^{-1}.$$

The contributions from the D-state wave function are clearly negligible relative to the S-state contributions.

Finally, consider the momentum-dependent part of $\mathcal{M}_d^{(b)}$. Here we make use of the integral parametrization

$$\frac{1}{\{(\vec{q}'-\vec{k})^2+M_\pi^2\}\vec{q}'^2} = \int_0^1 \frac{dz}{[\{(\vec{q}'-\vec{k})^2+M_\pi^2\}z+(1-z)\vec{q}'^2]^2}$$

$$= \int_0^1 \frac{dz}{(\vec{l}^2+m'^2)^2},$$

where $\vec{l}\equiv\vec{q}'-z\vec{k}$, $m'^2\equiv M_\pi^2 z(2-z)$, and $\vec{q}'=\vec{p}-\vec{p}'$. We can then write

$$\frac{\vec{J}\cdot(\vec{q}'-\vec{k})\vec{\epsilon}\cdot\vec{q}'}{\{(\vec{q}'-\vec{k})^2+M_\pi^2\}\vec{q}'^2}$$

$$= \int_0^1 dz \frac{(\vec{J}\cdot\vec{l})(\vec{\epsilon}\cdot\vec{l})+(z-1)(\vec{J}\cdot\vec{k})(\vec{\epsilon}\cdot\vec{l})}{(\vec{l}^2+m'^2)^2}. \quad \text{(D12)}$$

The second term vanishes in the pure S state. The Fourier transform of the first term is

$$\frac{(\vec{J}\cdot\vec{l})(\vec{\epsilon}\cdot\vec{l})}{(\vec{l}^2+m'^2)^2} = \frac{1}{8\pi}\int d^3r e^{-i\vec{l}\cdot\vec{r}}\left\{\frac{\vec{J}\cdot\vec{\epsilon}}{r}-(\vec{J}\cdot\hat{r})(\vec{\epsilon}\cdot\hat{r})\right.$$

$$\left.\times\left(\frac{1}{r}+m'\right)\right\}e^{-m'r}, \quad \text{(D13)}$$

which, in turn, yields the matrix element

$$\left\langle \frac{(\vec{J}\cdot\vec{l})(\vec{\epsilon}\cdot\vec{l})}{(\vec{l}^2+m'^2)^2} \right\rangle = \frac{1}{8\pi}\int d^3p\, d^3p'\, d^3r \phi_f(\vec{p}')$$

$$\times e^{-i(\vec{p}-\vec{p}'-z\vec{k})\cdot\vec{r}}f(\vec{r})e^{-m'r}\phi_i\left(\vec{p}-\frac{\vec{k}}{2}\right),$$

$$\text{(D14)}$$

where $f(\vec{r})\equiv(\vec{J}\cdot\vec{\epsilon}/r)-(\vec{J}\cdot\hat{r})(\vec{\epsilon}\cdot\hat{r})(1/r+m')$. Considering the pure S-state effect, we obtain

$$\left\langle \frac{\vec{J}\cdot(\vec{q}'-\vec{k})\vec{\epsilon}\cdot\vec{q}'}{\{(\vec{q}'-\vec{k})^2+m^2\}\vec{q}'^2} \right\rangle_{S \text{ state}} = \int_0^1 dz\left\langle \frac{(\vec{J}\cdot\vec{l})(\vec{\epsilon}\cdot\vec{l})}{(\vec{l}^2+m'^2)^2} \right\rangle_{S \text{ state}}$$

$$= \pi^2\int_0^1 dz\int d^3r \phi_f(\vec{r})(\vec{J}\cdot\vec{\epsilon})\frac{e^{-m'r}}{r}\exp[i(z-\tfrac{1}{2})\vec{k}\cdot\vec{r}]\phi_i(\vec{r}) - \pi^2\int_0^1 dz\int d^3r \phi_f(\vec{r})(\vec{J}\cdot\hat{r})(\vec{\epsilon}\cdot\hat{r})$$

$$\times\left(\frac{1}{r}+m'\right)e^{-m'r}\exp[i(z-\tfrac{1}{2})\vec{k}\cdot\vec{r}]\phi_i(\vec{r})$$

$$= \pi^2(\vec{J}\cdot\vec{\epsilon})\int_0^1 dz\int_0^\infty dr e^{-m'r}\frac{U^2}{r}\frac{\sin[(z-\tfrac{1}{2})kr]}{(z-\tfrac{1}{2})kr} - \pi^2(\vec{J}\cdot\vec{\epsilon})\int_0^1 dz\int_0^\infty dr e^{-m'r}U^2\left(\frac{1}{r}+m'\right)$$

$$\times\left\{\frac{\sin(z-\tfrac{1}{2})kr}{[(z-\tfrac{1}{2})kr]^3}-\frac{\cos(z-\tfrac{1}{2})kr}{[(z-\tfrac{1}{2})kr]^2}\right\}. \quad \text{(D15)}$$

Finally we obtain

$$\left\langle \frac{(\vec{J}\cdot\vec{q}'')\vec{q}'\cdot\vec{\epsilon}}{(\vec{q}''^2+M_\pi^2)\vec{q}'^2} \right\rangle_{S\ \text{state}} = \langle\vec{J}\cdot\vec{\epsilon}\rangle\ 0.747\ \text{fm}^{-1}, \tag{D16}$$

where we have used $k_{\text{th}}=0.685\ \text{fm}^{-1}$ (mass of π_0).

[1] S. Weinberg, Phys. Lett. B **251**, 288 (1990).

[2] S. Weinberg, Nucl. Phys. **B363**, 3 (1991).

[3] S. Weinberg, Phys. Lett. B **295**, 114 (1992).

[4] C. Ordóñez and U. van Kolck, Phys. Lett. B **291**, 459 (1992); C. Ordóñez, L. Ray, and U. van Kolck, Phys. Rev. Lett. **72**, 1982 (1994).

[5] U. van Kolck, Phys. Rev. C **49**, 2932 (1994).

[6] U. van Kolck, University of Washington Report No. DOE/ER/40427-13-N94, 1995.

[7] M. Rho, Phys. Rev. Lett. **66**, 1275 (1991).

[8] T.-S. Park, D.-P. Min, and M. Rho, Phys. Rep. **233**, 341 (1993).

[9] S. Weinberg, Physica **96A**, 327 (1979).

[10] Ulf-G. Meissner, Rep. Prog. Phys. **56**, 903 (1993).

[11] V. Bernard, N. Kaiser, and Ulf-G. Meissner, Int. J. Mod. Phys. E **4**, 193 (1995).

[12] R. Machleidt, K. Holinde, and Ch. Elster, Phys. Rep. **149**, 1 (1987).

[13] H. Georgi, Phys. Lett. B **240**, 447 (1990).

[14] E. Jenkins and A.V. Manohar, Phys. Lett. B **255**, 558 (1991).

[15] S.S. Kamalov, L. Tiator, and C. Benhold, Phys. Rev. Lett. **75**, 1288 (1995).

[16] V. Bernard, J. Gasser, N. Kaiser, and Ulf-G. Meissner, Phys. Lett. B **268**, 291 (1991).

[17] D. Drechsel and L. Tiator, J. Phys. G **18**, 449 (1992).

[18] P. de Baenst, Nucl. Phys. **B24**, 633 (1970); I.A. Vainshtein and V.I. Zakharov, Sov. J. Nucl. Phys. **12**, 333 (1971); Nucl. Phys. **B36**, 589 (1972).

[19] H.W.L. Naus, J.H. Koch, and J.L. Friar, Phys. Rev. C **41**, 2852 (1990).

[20] R. Beck *et al.*, Phys. Rev. Lett. **65**, 1841 (1990).

[21] E. Mazzucato *et al.*, Phys. Rev. Lett. **57**, 3144 (1986).

[22] A.M. Bernstein and B.R. Holstein, Commun. Nucl. Part. Phys. **20**, 197 (1991).

[23] V. Bernard, N. Kaiser, and Ulf-G. Meissner, Nucl. Phys. **B383**, 442 (1992).

[24] V. Bernard, N. Kaiser, J. Kambor, and Ulf-G. Meissner, Nucl. Phys. **B388**, 315 (1992); **B357**, 90 (1991).

[25] S. Scherer, J.H. Koch, and J.L. Friar, Nucl. Phys. **A552**, 515 (1993).

[26] V. Bernard, N. Kaiser, and Ulf-G. Meissner, Strasbourg Report No. CRN-94-62, hep-ph/9411287, 1994.

[27] P. Argan *et al.*, Phys. Rev. Lett. **41**, 629 (1978); Phys. Rev. C **24**, 300 (1981).

[28] J.H. Koch and R.M. Woloshyn, Phys. Rev. C **16**, 1968 (1977).

[29] P. Bosted and J. Laget, Nucl. Phys. **A296**, 413 (1978).

[30] G. Fäldt, Phys. Scr. **22**, 5 (1980).